

# Color Tuning in Rhodopsins: The Origin of the Spectral Shift between the Chloride-Bound and Anion-Free Forms of Halorhodopsin

Mikhail N. Ryazantsev,<sup>†</sup> Ahmet Altun,<sup>‡</sup> and Keiji Morokuma<sup>\*,†,§</sup>

<sup>†</sup>Cherry L. Emerson Center for Scientific Computation and Department of Chemistry, Emory University, Atlanta, Georgia 30322, United States

<sup>‡</sup>Department of Physics, Fatih University, 34500 B. Cekmece, Istanbul, Turkey

<sup>§</sup>Fukui Institute for Fundamental Chemistry, Kyoto University, 34-4 Takano Nishihiraki-cho, Kyoto 606-8103, Japan

**S** Supporting Information

**ABSTRACT:** Detailed knowledge of the molecular mechanisms that control the spectral properties in the rhodopsin protein family is important for understanding the functions of these photoreceptors and for the rational design of artificial photosensitive proteins. Here we used a high-level ab initio QM/MM method to investigate the mechanism of spectral tuning in the chloride-bound and anion-free forms of halorhodopsin from *Natronobacterium pharaonis* (phR) and the interprotein spectral shift between them. We demonstrate that the chloride ion tunes the spectral properties of phR via two distinct mechanisms: (i) electrostatic interaction with the chromophore, which results in a 95 nm difference between the absorption maxima of the two forms, and (ii) induction of a structural reorganization in the protein, which changes the positions of charged and polar residues and reduces this difference to 29 nm. The present study expands our knowledge concerning the role of the reorganization of the internal H-bond network for color tuning in general and provides a detailed investigation of the tuning mechanism in phR in particular.

The spectral and photochemical properties of rhodopsins, light-responsive seven-helix transmembrane proteins, have been the subject of intense studies for decades. This interest is motivated by the important role that these photoreceptors play in biophysical processes such as vision, ion transport, and phototaxis and by their use in nanotechnology and optogenetic applications.<sup>1,2</sup> Here we report the first ab initio multireference ONIOM [QM:MM (SORCI+Q//B3LYP/6-31g(d):AMBER-96)] investigation of the spectral properties of the halorhodopsin from *Natronomonas pharaonis* (phR). The results of this investigation not only revealed specific properties of this rhodopsin but also elucidated the mechanisms that control color tuning in rhodopsins in general.

While microbial rhodopsins (type-1 rhodopsins) and the visual pigments (type-2 rhodopsins) have different primary structures, their overall topologies are similar. Both types of rhodopsins consist of the retinal chromophore (PSB) and seven transmembrane helices that form an interior pocket for the chromophore. The chromophore, all-*trans*-retinal (PSBT) in microbial rhodopsins or 11-*cis*-retinal (PSB11) in the visual pigments, is covalently bound to the rest of the protein (opsin)

via a protonated Schiff base linkage. Photoisomerization of the retinal is the first step that triggers conformational reorganization in a surrounding protein environment and leads to signal transduction or ion transport. The electronic transition responsible for this photoisomerization is an optically active transition from the ground state to the first excited singlet state ( $S_0 \rightarrow S_1$ ). Experimental studies have shown that the absorption maxima ( $\lambda_{\max}$ ) corresponding to this transition vary over a wide range of wavelengths. This variation is possible because of the high sensitivity of the  $S_0 \rightarrow S_1$  transition in PSB to the protein microenvironment. The origin of the opsin shift, the spectral blue shift between  $\lambda_{\max}$  for the chromophore in the gas phase and in rhodopsins, has been the central question of color tuning for many years. The electrostatic effect of a protein environment was found to be the dominant factor that is responsible for the opsin shift.<sup>3</sup> The steric interaction of the chromophore with an opsin was shown to modify the spectral properties of visual rhodopsins by deforming the planar structure of the chromophore.<sup>3e,f,h</sup> In contrast, in bacteriorhodopsin (bR) and sensory rhodopsin II (sRII), the deviation from the planar structure was found to be negligibly small.<sup>3a</sup> To understand color tuning in rhodopsins, the electrostatic potential in the region of the PSB generated by an opsin can be decomposed into individual contributions from each amino acid. The most prominent contribution to the potential originates from the negatively charged residues (counterions) situated close to the <sup>+</sup>N-H part of the chromophore (one Glu in visual rhodopsins and two Asp's in bR and sRII). A number of theoretical<sup>3</sup> and experimental<sup>4</sup> studies have demonstrated that the counterions cause a prominent blue shift of the spectral band in going from the gas phase to the protein environment. In archaeal rhodopsins such as bR and sRII, the rest of an opsin (excluding the counterions) was shown to produce a red shift that partially counterbalances the effect of the counterions.<sup>3a</sup> The analogous red shift in Rh is still matter of debate.<sup>3c-e,5</sup>

Another important issue in the field is the need to elucidate the origin of the spectral shift between different rhodopsins (interprotein shifts). A recent QM/MM study of bR and sRII<sup>3a</sup> showed that two factors are essential for evaluating the 70 nm blue shift between these two rhodopsins: the composition of polar amino acids in the binding pocket (up to 5 Å from the

Received: January 28, 2012

Published: March 7, 2012

chromophore) and the reorganization of the internal H-bond network that changes the positions of the charged residues, the most important being the counterions. On the other hand, SAC-Cl QM/MM studies of the human red, green, and blue visual pigments revealed that the contribution from Glu113, the counterion, to the interprotein shifts between these rhodopsins is small.<sup>5</sup> However, in this case, a reorganization of the internal H-bond network leads to a change in the position of several polar residues located in the binding pocket. This reorganization was shown to contribute to the tuning (along with the amino acid composition and the deformation of the retinal). We recently showed that the H-bond network also regulates the optical properties of short-wavelength-sensitive visual rhodopsins.<sup>6</sup> Therefore, in all cases, the reorganization of the internal H-bond network has been found to be an important mechanism for controlling the spectral properties.

The recently published X-ray structures of the chloride-bound (phR-Cl)<sup>7</sup> and anion-free (phR-af)<sup>8</sup> forms of phR enable a computational investigation that complements the present knowledge of the molecular mechanisms of color tuning in rhodopsins. Experimental studies have shown that titration of the bound anion-free form of phR with a sodium chloride solution moves the  $\lambda_{\max}$  from 600 to 578 nm (Table 1).<sup>9</sup> Shortly after the discovery of phR, this 22 nm blue shift

**Table 1. First Vertical Excitation Energies and Absorption Wavelengths of phR-Cl and phR-af**

	vertical excitation energy (eV) [ $\lambda_{\max}$ (nm)]	
	phR-Cl	phR-af
experimental <sup>12</sup>	2.15 [578]	2.07 [600]
calculated	2.33 [532]	2.21 [561]

was attributed to the electrostatic effect of the chloride ion that supposedly moves from the solution to the <sup>+</sup>N-H region of the protein. Indeed, the X-ray structure<sup>7</sup> revealed that the chloride ion is situated in this region and thus should induce a blue shift. However, our investigation shows that the electrostatic effect of the chloride ion is only one of the contributing factors. Similar to bR and sRII or the visual pigments, the reorganization of the protein structure is also crucial for understanding the tuning mechanism. Moreover, since the two forms of phR differ in only one component (Cl<sup>-</sup>), the impact of the electrostatic effect of the Cl<sup>-</sup> can be clearly separated from the impact of the structural reorganization of the protein. From a theoretical perspective, these two proteins provide representative models for an investigation of the effect of the protein reorganization on the spectral properties of rhodopsins, an important factor that is still not completely understood. In the rest of this communication, we will give a detailed description of the tuning mechanisms in phR and discuss how this knowledge can be used to understand the molecular mechanisms that control the spectral properties of rhodopsins in general.

To construct the models, we started from the 2.0 Å X-ray structure (PDB entry 3A7K)<sup>7</sup> for phR-Cl and the 1.80 Å structure (3QBG) for phR-af.<sup>8</sup> The PROPKA<sup>10</sup> and PDB2PQR<sup>11</sup> programs in conjunction with visual inspection were used to assign protonation states of the titratable residues (pH 7) and add H atoms. The resulting structures were then optimized using two-layer ONIOM (QM:MM-EE) scheme. (QM = B3LYP/6-31G\*; MM = AMBER-96 for amino acids and Cl<sup>-</sup> and TIP3P for water; EE = electronic embedding)<sup>12</sup> as implemented in the Gaussian 09 package. To calculate the

spectral properties of the chromophore in the presence and absence of the protein environment (described as AMBER-96 point charges), we employed the SORCI+Q/6-31G\* level of theory as implemented in the ORCA 6.0 package,<sup>13</sup> which was successfully used to study the structure and spectroscopic properties of visual pigments in our previous work.<sup>3c,d</sup> Details are given in the Supporting Information (SI).

phR-Cl is composed of seven transmembrane  $\alpha$ -helices and the all-*trans*-15-*anti*-retinal chromophore. Negatively charged Asp252, Cl401, and three water molecules (wat502, wat503, and wat504) form a pentagonal H-bond cluster that is situated in the vicinity of the <sup>+</sup>N-H part of PSBT (Figure 1). Similar

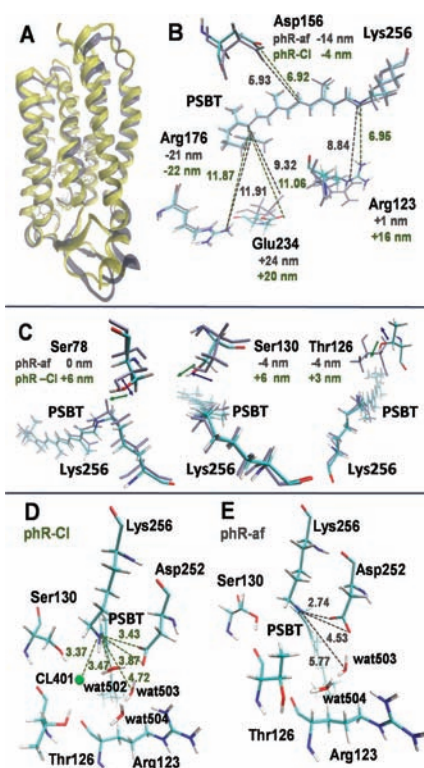


**Figure 1.** (A) Superposition of the QM/MM structures of phR-Cl (tan) and phR-af (gray). (B) Superposition of the QM/MM geometries and the contributions to  $\lambda_{\max}$  from the charged residues situated within 15 Å of the chromophore, excluding counterions. The geometries are shown in color for phR-Cl and in gray for phR-af. The contributions to  $\lambda_{\max}$  are shown in tan for phR-Cl and in gray for phR-af. (C) QM/MM geometries, contributions to  $\lambda_{\max}$ , the directions of the OH dipoles for three polar residues in the binding pocket that are found to significantly contribute to the tuning. The color code is the same as in (B). (D, E) H-bond network in the <sup>+</sup>N-H region of PSBT in the presence of a chloride ion (phR-Cl, D) and in phR-af (E).

clusters have been found in other bacterial rhodopsins such as bR and sRII, with the only difference being that Cl401 is replaced by a second Asp. Remarkably, the very recent X-ray structure of phR-af<sup>8</sup> revealed the pronounced difference relative to phR-Cl (Figure 1A–D). The main changes can be seen in the middle of helix C (in the region of the binding pocket; Figure 1A,E,D) and in the chloride uptake pathway. In phR-af, the side chain of Thr126, the residue in the middle of helix C that forms an H-bond with Cl401 in phR-Cl, occupies the place of this chloride ion. The water molecule that is H-bonded to Cl401 in phR-Cl (wat502) moves out from the cavity, and the remaining two water molecules change their positions (Figure

1D).  $\text{Cl}^-$  binding reorganizes the internal H-bond network of the protein, leading to a significant change in the position of the polar OH groups of Thr126, Ser78, and Ser130 and a smaller reorganization of other polar residues in the binding pocket. The five charged residues that fall into the region up to 15 Å from the chromophore (Asp252, Asp156, Arg176, Arg123, and Glu234) undergo a substantial rearrangement as well. As we will show, the polar residues in the binding pocket (up to 5 Å) and the charged residues up to 15 Å from the chromophore are essential for the color tuning, and the changes in their positions after the  $\text{Cl}^-$  binding contribute to the interprotein shift.

Another important structural effect that should be investigated is the change in the geometry of the chromophore in going from the gas phase to phR-af and then to phR-Cl. The geometry of a  $\pi$ -conjugated compound is sensitive to external electrostatic fields, which can change the lengths of single and double bonds by elongating the former and contracting the latter. This geometrical distortion can be quantified in terms of the bond length alteration (BLA), defined as the average difference between the lengths of the single and double bonds in the conjugated chain. The effect of the protein electrostatic field on the BLA in PSB was previously reported for bovine rhodopsin<sup>3c,d</sup> and archaeal rhodopsins such as bRh and sRII.<sup>3a</sup> These studies demonstrated that the BLA increases when PSB goes from the gas phase to the protein environment. Our results corroborate these findings. The calculated BLA in gas-phase PSBT (0.027 Å) increases to 0.045 Å in phR-af and to 0.064 Å in phR-Cl. To confirm that the origin of the BLA change is the polarization of the chromophore electron density by the protein environment, we reoptimized the models at the ONIOM (QM:MM-ME) level (ME = mechanical embedding with the RESP charges calculated for the gas-phase chromophore). In contrast to the EE scheme, the ME scheme neglects the reorganization of the electron density in the QM part caused by the MM part and treats the electrostatic interaction between them at the MM level. The PSBT BLAs at this level of theory are 0.024 Å for phR-Cl and 0.026 Å for phR-af, which are close to the gas-phase value (see the SI). In addition, we found that the deviation of the dihedral angles from those in the gas-phase planar structure is very small in both phR-af and phR-Cl (see the SI). Therefore, similar to bR and sRII, the main change in the geometry of the chromophore in going from the gas phase to the proteins is the change in BLA that originates from the electrostatic field of the opsin but not from the steric interactions.

The calculated absorption maxima of the retinal in the protein environment are in close agreement with experimental data (within 0.18 eV; Table 1). The blue shift between phR-af and phR-Cl observed experimentally (600 nm  $\rightarrow$  578 nm) is reproduced by our calculations (561 nm  $\rightarrow$  532 nm). To evaluate the mechanisms responsible for the opsin and interprotein shifts in phR, we carried out a series of model calculations. We created models that take into account the electrostatic effects of only part of the residues that are included in the original models. We kept the AMBER charges of the residues included in the corresponding model, set the charges of the rest of the opsin residues to zero, and performed a SORCI+Q calculation for each model. Thus, the model phR-Cl(PSBT) includes only the bare chromophore without any external charges; phR-Cl(PSBT+count) includes the charges of the counterions (Asp252 and Cl401); phR-Cl(PSBT+5.0Å) includes charges of all the residues that fall in the region within 5 Å of the chromophore (the counterions and 22 neutral and

polar residues; see the SI for a complete list); and phR-Cl(PSBT+5.0Å+chr) includes all of the charges from phR-Cl(PSBT+5.0 Å) plus the charges of the four charged residues situated within 15 Å of the chromophore (Arg123, Asp156, Arg176, and Glu234). The models for phR-af were constructed in the same way. Thus, phR-af(PSBT+count) includes the charges of Asp252, etc. The results of these calculations are shown in Figure 2. The residues included in the models phR-

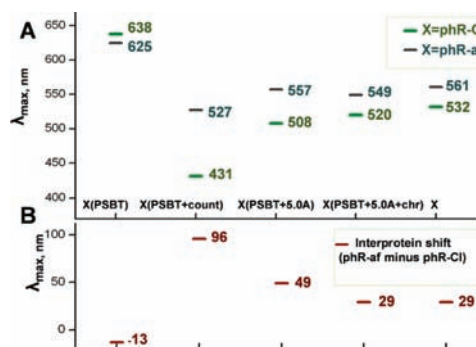


**Figure 2.** (A)  $\lambda_{\text{max}}$  for several models of phR-Cl (green) and phR-af (blue). (B) The interprotein shifts for the models.

Cl(PSBT+5.0 Å+chr) and phR-af(PSBT+5.0 Å+chr) are sufficient to obtain  $\lambda_{\text{max}}$  values that are within 12 nm of those calculated when charges of all residues are included (models phR-Cl and phR-af). The counterions (Asp252 for phR-af and Asp252 + Cl401 for phR-Cl) cause a prominent blue shift [models phR-Cl(PSBT+count) and phR-af(PSBT+count)]. This shift is larger in phR-Cl (638 – 431 = 207 nm) than in phR-af (625 – 527 = 98 nm). In both cases, the electrostatic field of the rest of the protein reduces the effect of the counterions. This leads to a red back-shift in both proteins, as was also found for bR and sRII.<sup>3a</sup> However, the magnitude of the shift in these two forms is different: 101 and 34 nm for phR-Cl and phR-af, respectively. This difference in the red back-shift explains the relatively small 29 nm net interprotein shift between phR-Cl and phR-af. Specifically, in phR-Cl, the electrostatic effect of Asp252 [model phR-Cl(PSBT+Asp252)] accounts for the 112 nm blue shift, which is slightly larger than the 98 nm blue shift calculated for phR-af [model phR-af(PSBT+count)]. The negative charge located on the chloride ion induces an additional 95 nm blue shift, resulting in a 96 nm interprotein shift between phR-af and phR-Cl. On the other hand, the residues up to 5 Å from the chromophore, excluding the counterions, reduce this shift to 49 nm. Finally, the presence of the additional four charged residues in the models phR-Cl(PSBT+5.0 Å+chr) and phR-af(PSBT+5.0 Å+chr) reduces the shift to 29 nm. As the next step, we estimated the influence of each polar residue in the binding pocket and the charged residues within 15 Å of the chromophore on the spectral properties by setting the charges of these residues to zero. We found that the impact of some residues on the spectral shift differs considerably for phR-Cl and phR-af. The contributions to  $\lambda_{\text{max}}$  from the three most significant polar residues of the binding pocket and the four charged residues are shown in Figure 1B,C. The contributions from all of the polar residues of the binding pocket can be found in the SI.

The spectral shift caused by the electrostatic field of a residue depends on the distance from this residue to the chromophore. A number of quantum-chemical calculations have demonstrated that shortening or elongation of the distance from a counterion



to the  $^+N-H$  region leads to a larger or smaller blue shift, respectively.<sup>14</sup> In pH-R-Cl, the reorganization of the H-bond network caused by  $Cl^-$  leads to a change in the position of Asp252 relative to that in pH-R-af. However, as shown in Figure 1D,E, the reorientation of the carboxyl group of Asp252 results in the shortening of the distance from the  $^+N-H$  group to one of the carboxyl oxygens and the elongation of the distance from  $^+N-H$  group to the other carboxyl oxygen. The effects of this reorganization partially cancel each other out and contribute 14 nm to the interprotein shift. In addition, the change in the orientation of the OH groups (dipole moments) of Ser78, Thr126, and Ser130 and the change in the position of Asp156 and Arg123 (charges) are found to affect the color tuning significantly. Figure 1C shows the positions of these residues, the directions of the dipole moments of the OH groups, and the contribution of these residues to the spectral shifts. For the polar residues (Thr126, Ser78, and Ser130), the change in the orientation and position of the OH groups leads to a significant difference in these contributions. Analogously, the changes in the distances from Asp156 and Arg123 to PSBT in going from pH-R-af to pH-R-Cl affect the contributions of these residues to  $\lambda_{max}$  (Figure 1B). The elongation of the distance from negatively charged Asp156 to the  $^+N-H$  part of the chromophore leads to a smaller negative impact of this residue on  $\lambda_{max}$  in pH-R-Cl ( $-4$  nm) than in pH-R-af ( $-14$  nm). Accordingly, the shortening of the distance from positively charged Arg123 results in a larger positive contribution of this residue in pH-R-Cl ( $+15$  nm) than in pH-R-af ( $+1$  nm). The two remaining residues (Arg176 and Glu234) contribute to  $\lambda_{max}$  significantly. However, their effects are similar in the two forms of pH-R and thus do not significantly affect the interprotein shift.

In conclusion, our theoretical investigation shows that the magnitude of the interprotein shift between pH-R-af and pH-R-Cl is controlled in two ways: directly via the electrostatic interaction of the chloride ion with the electron density of the chromophore and indirectly via a change in the position of the polar and charged residues of the protein induced by this chloride ion. Therefore, the composition and three-dimensional structure of this protein determine not only the opsin shift in pH-R-af and pH-R-Cl but also the interprotein shift between these two forms. These results can be utilized for the rational design of pH-R derivatives with different optical properties. Beyond pH-R, our study clearly shows that a change in the position of charged and polar residues caused by a reorganization of the H-bond network leads to a significant interprotein shift. Remarkably, a reorganization of charged residues situated even as far as 6–10 Å from the chromophore affects the tuning. For the short-wavelength-sensitive visual pigments, past experiments and our recent QM/MM study showed that mutations of residues situated far from the chromophore tune  $\lambda_{max}$  by modifying the H-bond network around the retinal.<sup>6</sup> The present study suggests that a distant mutation affecting the internal H-bond network in a protein can modify positions of not only counterions but also other charged residues, leading to a detectable spectral shift. This kind of long-range color-tuning mechanism may explain recent experiments showing that a single amino acid replacement in a distant cytoplasmic loop (A178R) of the proteorhodopsin causes a 20 nm red shift in  $\lambda_{max}$ .<sup>15</sup> Combined theoretical and experimental studies will further elucidate this mechanism of color tuning in retinal proteins.

## ■ ASSOCIATED CONTENT

### Supporting Information

Cartesian coordinates of the models and contributions to  $\lambda_{max}$  from the polar residues of the binding pocket. This material is available free of charge via the Internet at <http://pubs.acs.org>.

## ■ AUTHOR INFORMATION

### Corresponding Author

keiji.morokuma@emory.edu

### Notes

The authors declare no competing financial interest.

## ■ ACKNOWLEDGMENTS

The authors thank Prof. Shozo Yokoyama and Dr. Sivakumar Sekharan for useful discussions. The work at Emory was supported in part by NIH Grant R01EY016400-04 and that at Kyoto by a CREST grant from JST in the area of High Performance Computing. The authors also acknowledge NSF MRI-R2 Grant CHE-0958205 and the use of the resources of the Cherry Emerson Center for Scientific Computation.

## ■ REFERENCES

- (1) Palczewski, K. *Annu. Rev. Biochem.* **2006**, *75*, 743.
- (2) Hegemann, P.; Moglich, A. *Nat. Methods* **2011**, *8*, 39.
- (3) (a) Hoffmann, M.; Wanko, M.; Strodel, P.; Konig, P. H.; Frauenheim, T.; Schulten, K.; Thiel, W.; Tajkhorshid, E.; Elstner, M. *J. Am. Chem. Soc.* **2006**, *128*, 10808. (b) Hasegawa, J.-y.; Fujimoto, K. J.; Nakatsuji, H. *ChemPhysChem* **2011**, *12*, 3106. (c) Altun, A.; Yokoyama, S.; Morokuma, K. *J. Phys. Chem. B* **2008**, *112*, 16883. (d) Altun, A.; Yokoyama, S.; Morokuma, K. *J. Phys. Chem. B* **2008**, *112*, 6814. (e) Bravaya, K.; Bochenkova, A.; Granovsky, A.; Nemukhin, A. *J. Am. Chem. Soc.* **2007**, *129*, 13035. (f) Coto, P. B.; Strambi, A.; Ferre, N.; Olivucci, M. *Proc. Natl. Acad. Sci. U.S.A.* **2006**, *103*, 17154. (g) Schapiro, I.; Ryazantsev, M. N.; Ding, W. J.; Huntress, M. M.; Melaccio, F.; Andruniow, T.; Olivucci, M. *Aust. J. Chem.* **2010**, *63*, 413. (h) Fujimoto, K.; Hayashi, S.; Hasegawa, J.-y.; Nakatsuji, H. *J. Chem. Theory Comput.* **2007**, *3*, 605.
- (4) Sakmar, T. P.; Franke, R. R.; Khorana, H. G. *Proc. Natl. Acad. Sci. U.S.A.* **1989**, *86*, 8309.
- (5) Fujimoto, K.; Hasegawa, J.-y.; Nakatsuji, H. *Bull. Chem. Soc. Jpn.* **2009**, *82*, 1140.
- (6) Altun, A.; Morokuma, K.; Yokoyama, S. *ACS Chem. Biol.* **2011**, *6*, 775.
- (7) Kouyama, T.; Kanada, S.; Takeguchi, Y.; Narusawa, A.; Murakami, M.; Ihara, K. *J. Mol. Biol.* **2010**, *396*, 564.
- (8) Kanada, S.; Takeguchi, Y.; Murakami, M.; Ihara, K.; Kouyama, T. *J. Mol. Biol.* **2011**, *413*, 162.
- (9) Scharf, B.; Engelhard, M. *Biochemistry* **1994**, *33*, 6387.
- (10) Li, H.; Robertson, A. D.; Jensen, J. H. *Proteins* **2005**, *61*, 704.
- (11) Dolinsky, T. J.; Czodrowski, P.; Li, H.; Nielsen, J. E.; Jensen, J. H.; Klebe, G.; Baker, N. A. *Nucleic Acids Res.* **2007**, *35*, W522.
- (12) Cornell, W. D.; Cieplak, P.; Bayly, C. I.; Gould, I. R.; Merz, K. M.; Ferguson, D. M.; Spellmeyer, D. C.; Fox, T.; Caldwell, J. W.; Kollman, P. A. *J. Am. Chem. Soc.* **1995**, *117*, 5179.
- (13) Neese, F. *J. Chem. Phys.* **2003**, *119*, 9428.
- (14) Cembran, A.; González-Luque, R.; Altoè, P.; Merchán, M.; Bernardi, F.; Olivucci, M.; Garavelli, M. *J. Phys. Chem. A* **2005**, *109*, 6597.
- (15) (a) Yoshitsugu, M.; Shibata, M.; Ikeda, D.; Furutani, Y.; Kandori, H. *Angew. Chem., Int. Ed.* **2008**, *47*, 3923. (b) Yamada, K.; Kawanabe, A.; Kandori, H. *Biochemistry* **2010**, *49*, 2416.